International Journal of Climatology

Anomalies, trends and variability in atmospheric fields related with hailstorms in Northeastern Spain

Journal:	*International Journal of Climatology*
Manuscript ID:	JOC-13-0343
Wiley - Manuscript type:	Research Article
Date Submitted by the Author:	26-Jun-2013
Complete List of Authors:	García-Ortega, Eduardo; University of León, Hermida, Lucía; Universidad de León, Hierro, Rodrigo; Universidad Austral, Merino, Andrés; Universidad de León, Gascón, Estíbaliz; Universidad de León, Fernandez-Gonzalez, Sergio; Universidad de Leon, Fisica Sánchez, José Luis; Universidad de Leon, Fisica López, Laura; Universidad de Leon, Fisica
Keywords:	Hailstorms, Western Mediterranean, Anomalies, Trends, Morlet transform

Anomalies, trends and variability in atmospheric fields related with hailstorms in Northeastern Spain

García-Ortega E.[a], Hermida L.[a] , Hierro R.[b], Merino A.[a] , Gascón E.[a] , Fernández-González S.[a] , Sánchez JL.[a] , López L.[a]

[a] Atmospheric Physics Group. IMA, University of León, 24071-León, Spain.

[b] Facultad de Ingeniería, Universidad Austral, Buenos Aires, Argentina.

* Correspondence to: Eduardo García-Ortega. Atmospheric Physics Group. IMA, University of León, 24071-León, Spain.

E-mail: eduardo.garcia@unileon.es

Phone: +34 987 293 192

Abstract

Hailstorms become a serious meteorological risk in mid-latitudes countries and due to their local scale development and short time span, their forecast is still an open problem. Moreover, the lack of reliable hailstorm occurrence databases is an important handicap for NWP models validation, time trends studies and their relationships with global warming and climate change. However, this fact can be overcome by knowing the physical relationships between the favourable synoptic patterns and the mesoscale triggering factors for hailstorm development in every local study area.

Norteastern Spain is one of the European regions with more hailstorm days observed in summer months. Since 2001, from May to September, reliable databases of hailstorm occurrence in the Middle Ebro Valley have been recorded, knowing their intensity, time-frequency and spatial coordinates. June and July 2006 presented the highest number of hailstorm days ever observed in 2001-2010 period. With the objective of analysing the meteorological factors responsible for this anomaly, atmospheric patterns at low and mid-tropospheric levels were studied. A set of special synoptic configurations, with an evident deviation of climatic values were found, causing anomalies in 850 hPa temperature with respect to the characteristic values of the 2001-2010 and 1950-2010 periods. The analysis of the anomalies in relation to both periods of time has allowed to detect a positive trend in 850 hPa temperature and geopotential height in the Western Mediterranean area. As a consequence, the

characteristic synoptic circulation has been modified since 1950, changing towards low level patterns that favour adequate thermodynamic environments for hailstorm development in Northeastern Spain. Finally we have studied the periodicities in the monthly 850 hPa temperature field, after a previous cluster analysis, in order to improve the knowledge about the seasonal forecast of hailstorms.

Keywords

Hailstorms, Western Mediterranean, Anomalies, Trends, Morlet transform

1. Introduction

Hailstorms are defined as small-scale severe weather phenomena and are one of the most important meteorological risk in mid-latitude continental areas. In the Mediterranean and Southwestern Europe, summer month hailstorms provoke millions Euros in losses that are not restricted to agriculture, but rather, they affect industry, property, and occasionally cause loss of life.

Severe convection refers to the transfer of heat and humidity through a vertical flow associated with flotability, being able to generate adverse phenomena such as hail, tornadoes, intense precipitation and strong winds. Doswell (1987) and Houze (1993) established the mechanisms to get a pre-convective environment: atmospheric instability, low-level moisture and a trigger mechanism. The thermodynamic conditions that favour the onset of convection are well known, however, the detection and documentation of hailstorms is a very complicated

task because of its large spatial and temporal variability, and the fact that they are small-scale convective phenomena. For these reasons, the observation analysis and forecasting of hailstorms present important challenges, with the most important being the improvement of spatial and temporal precision, as well as the availability of a forecast with enough forewarning to minimize the damages.

The Northeastern (NE) Spain, specifically the Middle Ebro Valley (MEV, see fig. 1), is one of the areas in Europe with the highest occurrence of severe convective phenomena (Brooks *et al.*, 2003), along with the Alps and the Balkans. In some instances the storms have been severe, precipitating large-sized hail and causing important losses (García-Ortega *et al.*, 2007). The damage caused by hail amounts to around 100 million Euros per year, which indicates that hail precipitation is not only frequent but also has a major social and economic impact. Since 2001, the Atmospheric Physics Group (GFA) of the University of León (ULE) has carried out the detection and tracking of hailstorms in the MEV, during the period from May to September, using a nowcasting model with C-band radar (López and Sánchez, 2009; Sánchez *et al.,* 2013). Additionally, there is a vast hailpad network deployed and voluntary observers which help to verify where and when hail falls, as well as having relevant information, such as the size distribution or associated kinetic energy (Sánchez *et al.,* 2009). Additionally, the GFA has established two objective classifications at both, synoptic-scale (García-Ortega *et al.*, 2011) and mesocale (García-Ortega *et al.*, 2012; Merino *et al.*, 2013) defining the dynamic and

thermodynamic environments favourable to the onset and development of convection resulting in hail in the MEV.

In the last few years, different studies have been done trying to establish a relationship between the current climatic change scenario and its consequences in the intense precipitation events, hail or tornadoes. Warming of the climate system is unequivocal, as is now evident from observations of increases in global average air. In Southwestern Europe the increase in the surface temperature in the period 1970-2004 it is shown to be between 1 ºC – 2 ºC (IPCC, 2007). The question arises as to whether any evidence suggests an increase in hailstorm events either in number or intensity. Moreover, the lack of reliable surface observation systems is the main obstacle to know the trends in hailstorms occurrence. This fact makes this question difficult to answer.

However, different studies have contributed to understand the influence of climate change and the occurrence of thunderstorms and hail events. Leslie *et al.* (2008) using numerical climatic simulations showed that hailstorm severity, duration and paths are all sensitive to small changes in atmospheric parameters. Botzen *et al.* (2010) showed that projected climate change may lead to increase damage caused by hailstorms in the future. In particular the damage is expected to be large in climate change scenarios where global temperatures are expected to increase by up to 2 ºC by 2050.

Some authors have tried to find evidence of changes in hail precipitation.

Based on loss data of an agricultural insurance company in Switzerland (1920–1999), Schiesser (2003) reported a substantial increase in the number of hail events between 1980 and 1994. Piani *et al.* (2005) concluded that in Central Italy, a growing trend of summer hailstorm frequency has been detectable since the second half of the 1970s, and will likely be stationary or weakly growing in the future, being more evident in spring. Over Ontario, Canada, Cao (2008) identified a robust, ever-increasing frequency of severe hail events over the last decades using damage data. Kunz *et al.* (2009), based on insured building damage, observed in Germany that during the period 1974-2003, there was no increase in the number of thunderstorm days, however, there was an increase in the number of hailstorm days and also in the associated hail damage. Berthet *et al.* (2011) detected an increase in hail intensity by 70% during the 1989–2009 period, while the frequency did not change significantly. Mohr and Kunz (2013) found that the atmosphere has become more unstable over Central Europe over the last two to three decades.

In order to overcome the lack of observations, relationships between the hailstorm occurrence and the synoptic/mesoscale atmospheric patterns can be established. The observed trends or the anomalies in the atmospheric conditions should influence the occurrence of hailstorms, as well as their intensity. An understanding of connections between the synoptic atmospheric pattern trends and their effect on the formation of local thermodynamic regimes could improve the quality of seasonal forecasts.

Based on this idea, this paper is focused on two main objectives. The first one is to explain the meteorological anomalies that influenced the thermodynamic state of the atmosphere, causing an exceptional number of hailstorm days (HD) in June and July of 2006, in comparison with the period 2001-2010. The second one is to investigate if, in view of the anomalies found between atmospheric patterns of 2006 and the 2001-2010 and 1950-2010 periods, there is a significant trend in the time evolution of the representative variables that allow us to establish conclusions about the trends and the periodicities of hailfalls in Southwestern Europe.

The paper is organised as follows: in section 2 we present the methodology and the databases. In section 3 we examine and discuss the results obtained about atmospheric patterns, anomalies, trends and their significance, the decadal rates of change and periodicities of the selected study fields. In section 4 we present the conclusions.

2. Methodology and databases

A high-time resolution C-band radar from the GFA is deployed at 10 km to the SW of Zaragoza city. This radar makes the tracking and the study of time and spatial development of hailstorms in a radius of, approximately, 140 km (fig. 1). The GFA has developed a nowcasting model for the detection of hail (López and Sánchez, 2009; Sánchez *et al.,* 2013) with a resolution of 1x1x1 km^3. Twelve elevation angles are used and the information registered is updated every 3.5 minutes. The short lifetime of hail events and their local occurrence

make the detection and study of hailstorms very difficult (Smith and Waldvogel, 1989). For this reason, the GFA also has a network of 729 observers in the study area. The information coming from the observers, along with the model outputs, has allowed us to know the number of hailstorms, their intensity, evolution and structure, as well as their spatial distribution during the period 2001-2010.

The annual distribution of hail days corresponding to the period 2001-2010 is shown in Fig. 2. The maximum number of HD is 50 in 2006, whereas the average value is 32.6 days. The period analyzed each year corresponds to the months from May to September. Throughout this period, there is an important climatic variability that leads to notable variations in temperature at mid-latitudes, which influences the intensity of the troughs, ridges, and the intensity and extension of cold and warm air masses. For this reason, the data has been classified by month for each of the years of the study. The results are shown in Table 1.

As can be seen, in June and July 2006, more than half of the days of the months were HD. This anomaly prompted us to study the atmospheric characteristics of June and July 2006, and their comparison with the representative values corresponding to the period 2001-2010 (with registered HD data), and from the period 1950-2010 in order to find possible trends.

The atmospheric conditions of the study area have been characterised by the

monthly 1950-2010 gridded reanalysis data from the National Centers for Environmental Prediction (NCEP), with a latitude–longitude resolution of 2.5º x 2.5º (Kalnay *et al.*, 1996). The selected area comprises from 30ºN to 50ºN of latitude and from 20ºW to 10ºE of longitude, covering Southwestern Europe, Northwestern Africa (the Western Mediterranean area) and the mid-latitude Eastern Atlantic Ocean. The window dimensions were selected, not only in an effort to be consistent with the objectives of this study, but also to avoid the influence of circulation features in regions outside the study area. The dynamic and thermodynamic state of the atmosphere was described by the temperature and the geopotential height at 850 hPa and 500 hPa (T850, T500, G850 and G500). These fields provide relevant information about the atmospheric status at low and mid-tropospheric levels.

Additionally, the anomalies for T850 with respect to the periods 2001-2010 and 1950-2010, in the months of June and July, were calculated. In view of the results, we have obtained, on a cell-by-cell basis, the T850 and G850 trends using the Mann-Kendall test, as well as its significance. This test allows us to statistically determine if the values of a variable increase or decrease over time. The rate of change of the variables was found using the Sen method, a non-parametric estimator of trend magnitude robust to outliers (Sen, 1968). The calculations were done using the MAKESENS application from the Finnish Meteorological Institute (Salmi *et al.*, 2002). The slope obtained by the Sen method, in each of the matrix points, was used to estimate the decadal rates of change (Beier *et al.*, 2012).

Once the trends were obtained and the T850 (not shown) and G850 fields in the period 1950-2010 were studied, a cluster analysis (CA) was performed with the original values of T850 as a useful way of objectively organising these patterns into groups. Using years as variables and the grid-points as cases, the CA allowed us to establish grouping structures on the matrix for the selected atmospheric fields. The non-hierarchical k-means method (Anderberg, 1973) was used, and the Euclidean distance was taken as the similarity index. Gong and Richman (1995) showed that non-hierarchical methods outperformed hierarchical techniques. This method minimises the sum of the intragroup sum of squares (D), which decreases as the number k of groups increases. The cluster number needs to be identified before the algorithms can proceed, selecting the optimum number when the decrease in D was not significant.

Nevertheless, the decision regarding the number of groups is not a completely objective task as a degree of subjectivity is present, based on the physical evidences. The spatial structure of the decadal rates of change of the temperature and geopotential height is a correct reference to give a physical interpretation for the results of the CA and select the most appropriate number of clusters.

With the objective of studying the possible periodicities present in the T850 field, and using the CA results, a wavelet analysis was carried out. The Continuous Wavelet Transform (CWT) analysis is a powerful tool for studying

multi-scale and non-stationary processes occurring over finite spatial and temporal domains (Lau and Weng, 1995). This implies a substantial advantage with respect to the Fourier transform, whose analysis is limited to stationary signals and implies a loss of information in the temporal domain.

Its development began with Morlet (1983) and, since then, different applications in the field of Earth sciences have been found (Labat, 2005; Sang, 2013). The Morlet wavelet has been used as a non-orthogonal and complex mother wavelet, which consists of a flat wave modified by a Gaussian envelope. This wavelet is subjected to a process of dilation and translation along the studied signal to obtain the wavelet coefficients. The wavelet function (Ψ_0) depends on a time variable (η) with zero mean and localised in a time-frequency space (Torrence and Compo, 1998). This function is defined as:

$$\psi_0(\eta) = \pi^{-1/4} e^{i\omega_0\eta} e^{-\eta^2/2}$$

where ω_0 is the non-dimensional frequency with a value of 6, which satisfies the the admissibility condition (Farge, 1992). The different advantages of the wavelet analysis have allowed us to study the variability of the time series, taking account of the temporal dimension and reaching a compromise in the localization of a signal in a time-frequency space.

3. Results.

3.1. Synoptic patterns.

Figure 3 shows the geopotential height maps at 850 hPa. During the period 1950-2010, June and July patterns were similar, and were characterized by a flow from the West, with a small undulation over the Iberian Peninsula (IP). To the West and to the East, the Azores High and a high-pressure center located over the East of Algeria can be found. However, in the period 2001-2010 the undulation becomes deeper, causing a trough over the West of the IP. In 2006 the trough, whose axis is to the West of Portugal, is well-formed leading to an embedded low in June, to the SW of the IP. These patterns change the low level wind over the NE Spain causing a South component flow, which produces the transport of warm and humid air from the Mediterranean Sea.

The 1950-2010 average pattern at 500 hPa (Fig. 4) is characterised by a zonal flow with a light undulation forced by the high pressure center from the North of Africa. The configuration of the period 2001-2010 is similar, although the geopotential values over the IP are slightly higher. However, 2006 shows a trough that penetrates through the West of the IP as an extension of what was observed at 850 hPa.

Precisely, the patterns observed in 2006 create favourable synoptic conditions for the formation of hailstorms in the MEV, according to the cluster classification done by García-Ortega *et al.* (2011). These synoptic patterns are associated with the entrance of cold fronts that cause atmospheric instability, leading to storm formation that are sometimes prefrontal. The presence of a trough with or without an embedded low at 850 hPa is a common characteristic in hail risk

situations in the MEV. This synoptic pattern always appears in the SW of the study area.

The temperature field is associated with the geopotential height. The presence of troughs or lows is related to the entrance of cold air masses, which, when extended in height, provoke unstable situations. On the other hand, the MEV is a region in which, during the summer months, the high temperatures favour the formation of thermal mesolows (Tudurí *et al.*, 2003; García-Ortega *et al.*, 2007) that, along with an adequate low-level wind pattern, can lead to one of two possibilities. The first is the formation of areas with strong convective instability, and the second is the appearance of convergence areas. Both factors are the main ingredients for the triggering convection associated with hail events (García-Ortega *et al.*, 2012). Figure 5 shows the differences in temperature at 850 hPa with respect to the two studied series. Upon seeing the results, it is evident that there is an increase in temperature in June and July of 2006 that affects especially the NE of Spain, although the geometry of the isotherms is different. In June, the area with maximum positive differences respect to the 1950-2010 period (2.5 ºC – 3.0 ºC) covers the N and E of the Peninsula, while in July, the maximum positive differences are centered over France, with 2.0 ºC - 3.5 ºC over the NE of Spain.

3.2 Anomalies in June and July 2006.

Given the importance that the difference in temperature between low and mid-tropospheric levels has in the onset of convection, anomalies have been

calculated for the difference in temperature at 850 hPa and 500 hPa, using the standardised matrix data. For each grid-point in the domain, the average value, $\bar{x}$, and the standard deviation, σ, have been calculated. Those values that are outside of the interval defined by $\bar{x} \pm \sigma$, are considered to be significant anomalies.

Positive anomalies are shown in June and July of 2006 with respect to the period 2001-2010 (fig. 6 left). In June, there is an anomaly in the Mediterranean with maximum values of 2.8 ºC - 3.2 ºC, over Sardinia Island. Over the Atlantic, to the NW of Galicia, there is also an anomaly of 0.8 ºC -1.2 ºC. With respect to the period from 1950-2010, the anomaly is more evident, covering the Eastern of the IP (with values 1.6 ºC - 2.4 ºC) and extending toward the Mediterranean Sea (with maximum of 3.6 ºC – 4.0 ºC) and toward the Atlantic Ocean (fig. 6 top, right). In both cases, the anomalies are due to the increase in temperature at 850 hPa in the Mediterranean and to the N of the IP.

During the month of July 2006, anomalies with respect to the two series considered were observed, being centered in the SW of France (with maximum values of 3.2 ºC - 3.6 ºC), affecting almost all of the IP, with values of 2.0 ºC - 2.8 ºC in the MEV, with respect to both series. The anomaly in the period from 1950-2010 extends over the SE of the IP, reaching the North of Africa.

These anomalies are mainly due to the increase observed in the T850. It has been observed that there are not significant differences in the T500 values with

respect to the two periods in the study (not shown). If similar differences to those registered at 850 hPa had been observed, the difference in temperature between low and mid-levels would not provide any relevant information. Another noticeable fact is that more intense anomalies of T850 are observed with respect to the period 1950-2010 than respect to the period 2001-2010. These results suggest the possibility of an up trend of T850 in the study area.

3.3 Trends and cluster classification in the period 1950-2010.

We have obtained the T850 and G850 trends as well as its significance levels, for the period 1950-2010, using the Mann-Kendall test. Figs. 7 and 8 show the decadal rate of change obtained using the Sen method, and the level of significance for the Mann-Kendall test. Except for some of the grid-points where slight negative trends were found, in practically all of the study area, a positive decadal rate of change was observed for T850, which affects all of the Iberian Peninsula with maximum values in the Western Mediterranean, as well as the coast of Southeastern Spain. In these areas, the values exceed 0.5 ºC. decadal^{-1} and 0.4 ºC. decadal^{-1} in the months of June and July, respectively (fig. 7), with a level of significance $\langle \delta$ 0.001. The G850 (fig. 8) shows positive decadal rate of change in both months as well. The maximum values are found over the Eastern part of the study area, being 6 m. decadal^{-1} (June) and 5 m. decadal^{-1} (July). The level of significance is, in general, lowest in the areas affected by the maximum decadal rates of change (1 - $\langle$ > 0.95).

The existence of a positive T850 trend is evident in the period 1950-2010 in the

Mediterranean area close to the coast of Spain. This increase comes from the strengthening of the African ridge in the months of June and July, as shown in Fig. 8. As a consequence of this strengthening, a double-effect is produced: the cited increase of temperature at 850 hPa to the SE of Spain, especially during the month of June, which could be up to 3º between 1950-2010, and the wind pattern associated with the strengthening of the African ridge. The increase in temperature affects the low troposphere situated in the area over the Mediterranean Sea. This fact causes an increase in the water vapor content in the area. The wind pattern associated with the perturbation observed at G850 reinforces the southern component of low-level wind in the area, favouring a humid and warm air advection from the Mediterranean Sea to the East of the IP. This wind pattern, along with the orographic characteristics of the study area, facilitates the formation and development of convection in the MEV (García-Ortega *et al.,* 2012).

Thus, a reinforcement of this structure from the period 1950-2010 could cause an increase in the frequency of HD in the MEV. The absence of reliable data about hail in the second half of the 20th century does not allow us to know about the real data of the time evolution of the number of HD since 1950, however, the results of the study allow us to affirm that a positive trend in T850 and G850 is occurring, toward patterns that generate favourable environments for the development of hailstorms in NE Spain. The results are coherent with the observed fact that the anomalies from 2006 are deeper with respect to the period 1950-2010 than with respect to the period 2001-2010. In this context, the

anomaly observed in 2006 is an extreme case for this evolution pattern.

After confirming the T850 positive trend over the Western Mediterranean Sea, it was interesting to study the possible periodicities. However, before doing this study, we have analysed the groups that can be established between grid-points, taking the T850 time series. In order to do this, a cluster analysis was done for the original T850 data, using the methodology previously described. Based on the similarity criterion and the identification of the clusters with the structures observed in the decadal rate changes, and the T850 patterns from the period 1950-2010 (not shown), two clusters were selected for each month, June and July (fig. 9). From this result, and taking each cluster individually, we have studied the periodicities present in the time series of T850.

3.4 Wavelet analysis.

As it was explained in section 2, the wavelet analysis allows to study the variability of the time series taking account of the temporal dimension. With the objective of studying the periodicities in the cluster average temperature in the months of June and July from 1950 to 2010, a CWT was applied. Although linear tendencies do not affect the CWT results, the original time series were detrended, since as it was mentioned by Yi and Shu (2012), it is known that temperature data are composed by a linear trend, periods and a random signal.

Figure 10 shows the results for the CWT, along with the time series in each case of study. In cluster 1 of June one mode at around 20 years seems to

persist for the whole period. Another cycle of 7 years is presented, but after 1980 an abrupt change in frequency gives place to an oscillation mode at around 8-9 years that persists during the remaining time. Between 1970 and 1980 it is possible to detect the shortest wave of the time series, with a period of 2.5 years. With respect to cluster 1 of July, the largest wave seems to present, since year 1970 up to year 2010, a progressive change in frequency joint with a frequency modulation effect. This period shows increasing wavelengths with time, reaching a 30 years period at year 2010. By the other hand, lower wavelengths are more variable, with the presence of an oscillation mode with a period between 5-7 years since 1960 lasting to 1990. Then, a frequency change takes place, giving rise to wavelengths of period around 2.5 years, between 1990 and the end of the signal. For cluster 2 in June, a wavelength of period close to 27 years is distinguished for the first half of the signal. In addition, it is observed a prevailing oscillation mode of a period around 15-17 years during the whole time series. As in the previous cases, higher frequency waves are also important for the series, being possible to recognise for this wavelength range: one mode of period around 7.5 years, which starts in 1950 and suffers a frequency change close to 1970, increasing the wavelength in 1-2 years up to 2010; and another period at around 2.5-3 years, which appears suddenly during 1950 and 1990, lasting in both cases for 5 years. In cluster 2 July it is possible to decompose the signal in four wavelength ranges. The larger starts in 1960 showing a period of 27.5 years and, after a frequency change between 1970 and 1980, stays up to the end with a period of around 22.5 years. Another present structure from the initial time is a wave with a period of 10 years. A

slightly frequency modification is observable after 1980, decreasing the original wavelength to a period of 8 years. Other important range mode corresponds to a period of 6-7 years between 1950-1975, when a frequency change gives place to a wave of around 3-4 years. Finally, the lower wavelength range corresponds to 2.5-3 years which is perceptible along the whole study period.

4. Discussion and conclusions

The GFA from the University of León in Spain has access to a complete database for all of the hailstorms that happened in the MEV since 2001, between the months of May and September. In June and July 2006, there were an exceptionally high number of hailstorms in the MEV. Specifically, 33 HD were registered, these being 66% of the hailstorms from May-September 2006 and 74% more than in June and July 2010, the year with the second-highest number of hailstorms in these months. Because of this information, the characteristics of synoptic models in both months were studied, along with their differences with respect to the periods 2001-2010 and 1950-2010.

The selected domain ranges from 30ºN to 50ºN and 20ºW to 10ºE. Hailstorms are convective events; therefore, the selected atmospheric fields were temperature and geopotential height at 850 hPa and 500 hPa, corresponding to gridded re-analysis data from the NCEP. The synoptic patterns of June and July 2006 show important differences with respect to the patterns for the two cited periods. Specifically, at 850 hPa, there is a deepening of the trough located to the West of the Iberian Peninsula, which extends to 500 hPa, and that, along

with the reinforcement of high pressure centered in Algeria, generates a South-component flow over the NE of Spain.

Additionally, in 2006, there were positive anomalies in the difference of temperature at low and mid-tropospheric levels, due to the increase in temperature at 850 hPa. The anomalies, with respect to the period 2001-2010 reach 2.8 ºC - 3.2 ºC in June over Sardinia and 3.2 ºC - 3.6 ºC in July over SW France. These anomalies deepen when they are calculated with respect to the period 1950-2010, these being de 3.6 ºC - 4.0 ºC in June and extending over the Eastern coast of Spain in both months.

As such, trends in temperature and geopotential height at 850 hPa during this last period have been studied. A positive trend was found, with a decadal rate of change of T850 over de Peninsula, with maximum values of 0.5 ºC. decadal^{-1} and 0.4 ºC. decadal^{-1} in the months of June and July, respectively, in the Western Mediterranean, with a level of significance $\langle \delta$ 0.001. The G850 shows positive decadal rate of change in both months as well, being the maximum values of 6 m. decadal^{-1} (June) and 5 m. decadal^{-1} (July) over the Eastern part of the study area.

These results show a change in the atmospheric characteristics at 850 hPa between 1950 and 2010, and imply a strengthening of the African ridge during this period. This evolution causes the positive trend in T850 in the area affected by the ridge, with a maximum increase of 3ºC in the period 1950-2010 in T850-

June, over the Western Mediterranean. The increase of T850 and the deepening of the ridge generate winds with a strong Southern component over the MEV, with high water vapor content, which provide favourable environments for the development of convection and, specifically, an increase in the number of HD.

Once the trends and the decadal rates of change of the selected fields were studied, the periodicity of the T850 signal during the period 1950-2010 was analysed. Given the existing direct relationship between the results found for T850 and G850, T850 was selected for the next stage of investigation. Previously, a CA for the T850 field was done, using years as variables and the grid-points as cases for the period 1950-2010. The results show two very similar clusters for June and July, respectively. Cluster 1 includes the Northern half and the extreme SW of the study domain and cluster 2 includes the extreme S and SE.

We have obtained the periodicities of the mean 850 hPa temperature during 1950-2010, applying CWT over each cluster of June and July. In cluster 2 for both months, there are a greater number of cycles. Generally, there is a small cycle in 2.5 years, which reaches 3 years in cluster 2 in both months. In June, there is a greater cycle of 7 years in cluster 1 and of 7.5 years in cluster 2, changing in time to periods of 9 to 9.5 years, respectively. In July, these periodicities seem to be smaller beginning in general between 5 and 7 years, and decreasing in both cases.

In cluster 2 there is a new periodicity of 15-17 years in June; while in July it is close to 10 years, and diminishes to 8 years at the end of the series.

In all of the cases, greater periodicities that are relatively clear can be observed, except in the case of cluster 1 in July. The periodicities vary from 20 years in cluster 1 in June up to about 27 years in cluster 2. And in cluster 2 of July a cycle of 27.5 years descends to 22.5 also in the half of the time series.

The anomaly in 2006 is also seen in the time series of T850 (fig. 10). In cluster 1 June, the CWT shows a possible effect of the superposition of two cycles described, which could be responsible for the high number of HD. Similarly, this occurs in 1980, though we do not have data from this year. One can sense the superposition of cycles in cluster 1 for July, although it is not observed with the same clarity, due to the increase in the high values of periodicity of this cluster.

The results show a clear change in the temperature and geopotential fields at low tropospheric levels since 1950, affecting the Western Mediterranean area. This change generates synoptic environments that are more favourable to the development of hailstorms in NE Spain, which causes an increase in the number of HD. The periodicities of the mean 850 hPa temperature during 1950-2010 help to explain the anomaly observed in 2006, and show the importance of a more detailed analysis of the periodicities of the temporal series. Later studies will allow us to establish relationships between the periodicity found and

other factors, such as the NAO, solar radiation, solar activity or sunspot cycles, with the subsequent improvement in the seasonal forecasting of hailstorms.

Acknowledgments

The study was supported by the Plan Nacional de I+D of Spain, through the grant CGL2010-15930 and the Junta de Castilla y León through the grant LE176A11-2. The authors are grateful to Rocío Manjón for his help with data processing.

References

Anderberg MR. 1973. Cluster analysis for applications. Academic Press, New York. 359pp.

Beier CM, Signell SA, Luttman A, DeGaetano AT. 2012. High-resolution climate change mapping with gridded historical climate products. *Landscape Ecology* **27**: 327-342.

Berthet C, Dessens J, Sanchez JL. 2011. Regional and yearly variations of hail frequency and intensity in France. *Atmospheric Research* **100**: 391-400. DOI: 10.1016/j.atmosres.2010.10.008.

Botzen WJW, Bouwer LM, van den Bergh JCJM. 2010. Climate change and hailstorm damage: Empirical evidence and implications for agriculture and insurance. *Resource and Energy Economics* **32**: 341-362. DOI: 10.1016/j.reseneeco.2009.10.004.

Brooks HE, Lee JW, Craven JP. 2003. The spatial distribution of severe thunderstorm and tornado environments from global reanalysis data. *Atmospheric Research* **67–68**: 73-94. DOI: 10.1016/S0169-8095(03)00045-0.

Cao Z. 2008. Severe hail frequency over Ontario, Canada: Recent trend and variability. *Geophysical Research Letters* **35**: - L14803. DOI: 10.1029/2008GL034888.

Doswell III CA. 1987. The distinction between large-scale and mesoscale contribution to severe convection: A case study example. *Weather and Forecasting* **2**: 3-16. DOI: 10.1175/1520-0434(1987)002<0003:TDBLSA>2.0.CO;2.

Farge M. 1992. Wavelet transforms and their applications to turbulence. *Annual Review of Fluid Mechanics* **24**: 395-458. DOI: 10.1146/annurev.fl.24.010192.002143.

García-Ortega E, Fita L, Romero R, López L, Ramis C, Sánchez JL. 2007. Numerical simulation and sensitivity study of a severe hailstorm in northeast Spain. *Atmospheric Research* 83: 225-241. DOI: 10.1016/j.atmosres.2005.08.004

García-Ortega E, López L, Sánchez JL. 2011. Atmospheric patterns associated with hailstorm days in the Ebro Valley, Spain. *Atmospheric Research* **100**: 401-427. DOI: 10.1016/j.atmosres.2010.08.023.

García-Ortega E, Merino A, López L, Sánchez JL. 2012. Role of mesoscale factors at the onset of deep convection on hailstorm days and their relation to

the synoptic patterns. *Atmospheric Research* **114–115**: 91-106. DOI: 10.1016/j.atmosres.2012.05.017.

Gong X, Richman MB. 1995. On the application of cluster analysis to growing season precipitation data in North America east of the Rockies. *Journal of Climate* **8**: 897-931. DOI: 10.1175/1520-0442(1995)008<0897:OTAOCA>2.0.CO;2

Houze R. 1993. *Cloud Dynamics*, 573 pp. Academic Press, San Diego, California.

IPCC. 2007. Climate Change 2007: Synthesis Report. Contribution of Working Groups I, II and III to the Fourth Assessment Report of the Intergovernmental Panel on Climate Change. [Core Writing Team, Pachauri, R.K and Reisinger, A. (eds.)]. IPCC, Geneva, Switzerland, 104 pp.

Kalnay E, Kanamitsu M, Kistler R, Collins W, Deaven D, Gandin L, Iredell M, Saha S, White G, Woollen J. 1996. The NCEP/NCAR 40-year reanalysis project. *Bulletin of the American Meteorological* Society **77**: 437-471. DOI: 10.1175/1520-0477(1996)077<0437:TNYRP>2.0.CO;2.

Kunz M, Sander J, Kottmeier C. 2009. Recent trends of thunderstorm and hailstorm frequency and their relation to atmospheric characteristics in

southwest Germany. *International Journal of Climatology* **29**: 2283-2297. DOI: 10.1002/joc.1865.

Labat D. 2005. Recent advances in wavelet analyses: Part 1. A review of concepts. *Journal of Hydrology* **314**: 275-288. DOI: 10.1016/j.jhydrol.2005.04.003.

Lau K, Weng H. 1995. Climate signal detection using wavelet transform: How to make a time series sing. *Bulletin of the American Meteorological* Society **76**: 2391–2402. DOI: 10.1175/1520-0477(1995)076<2391:CSDUWT>2.0.CO;2

Leslie LM, Leplastrier M, Buckley BW. 2008. Estimating future trends in severe hailstorms over the Sydney Basin: A climate modelling study. *Atmospheric Research* **87**: 37-51. DOI: 10.1016/j.atmosres.2007.06.006.

López L, Sánchez JL. 2009. Discriminant methods for radar detection of hail. *Atmospheric Research* 93: 358-368. DOI: 10.1016/j.atmosres.2008.09.028.

Merino A, García-Ortega E, López L, Sánchez JL, Guerrero-Higueras AM. 2013. Synoptic environment, mesoscale configurations and forecast parameters for hailstorms in Southwestern Europe. *Atmospheric Research* **122**: 183-198. DOI: 0.1016/j.atmosres.2012.10.021.

Mohr S, Kunz M. 2013. Recent trends and variabilities of convective parameters relevant for hail events in Germany and Europe. *Atmospheric Research* **123**: 211-228. DOI: 10.1016/j.atmosres.2012.05.016.

Morlet J. 1983. Sampling theory and wave propagation. NAO ASI Series FI, Springer, p 233-261.

Piani F, Crisci A, De Chiara G, Maracchi G, Meneguzzo F. 2005. Recent trends and climatic perspectives of hailstorms frequency and intensity in Tuscany and Central Italy. *Natural Hazards and Earth System Science* **5**: 217-224. DOI: 10.5194/nhess-5-217-2005.

Salmi T, Maatta A, Anttila P, Ruoho-Airola T, Amnell T. 2002. Detecting trends of annual values of atmospheric pollutants by the Mann–Kendall test and sen's solpe stimates — the excel template application MAKESENS. Helsinki, Finnish Meteorological Institute Report No. 31. Helsinki, p. 35.

Sánchez JL, Gil-Robles B, Dessens J, Martin E, Lopez L, Marcos JL, Berthet C, Fernández JT, García-Ortega E. 2009. Characterization of hailstone size spectra in hailpads networks in France, Spain and Argentina. *Atmospheric Research* **93**: 641-654. DOI: 10.1016/j.atmosres.2008.09.033

Sánchez JL, López L, García-Ortega E, Gil B. 2013. Nowcasting of kinetic energy of hail precipitation using radar. *Atmospheric Research* **123**: 48-60. DOI: 10.1016/j.atmosres.2012.07.021

Sang Y. 2013. A review on the applications of wavelet transform in hydrology time series analysis. *Atmospheric Research* **122**: 8-15. DOI: 10.1016/j.atmosres.2012.11.003.

Schiesser H. 2003. Hagel. *Extremereignisse und Klimaänderung. Organe consultatif sur les changements climatiques (OcCC),* Bern, Swiss, pp. 65–68.

Sen PK. 1968. Estimates of the regression coefficient based on Kendall's tau. *Journal of the American Statistical Association* **63**: 1379-1389. DOI: 10.1080/01621459.1968.10480934

Smith PL, Waldvogel A. 1989. On determinations of maximum hailstone sizes from hailpad observations. *Journal of Applied Meteorology*. **28**: 71–76. DOI: 10.1175/1520-0450(1989)028<0071:ODOMHS>2.0.CO;2

Torrence C, Compo GP. 1998. A practical guide to wavelet analysis. *Bulletin of the American Meteorological Society* **79**: 61-78. DOI: 10.1175/1520-0477(1998)079<0061:APGTWA>2.0.CO;2

Tudurí E, Romero R, López L, García, E., Sánchez JL, Ramis C. 2003. The 14 July 2001 hailstorm in northeastern Spain: diagnosis of the meteorological situation. *Atmospheric Research*. **67–68:** 541–558.

Yi H, Shu H. 2012. The improvement of the Morlet wavelet for multi-period analysis of climate data. *Comptes Rendus Geoscience* **344**: 483-497. DOI: 10.1016/j.crte.2012.09.007.

	May	June	July	August	September	Total
2001	1	0	9	6	4	20
2002	2	4	7	6	4	23
2003	2	6	10	10	1	29
2004	2	6	11	14	4	37
2005	1	10	5	8	5	29
2006	5	17	16	4	8	50
2007	7	8	6	9	4	34
2008	6	6	11	15	1	39
2009	6	6	5	9	1	27
2010	1	9	10	10	6	36

Table 1. Monthly distribution of HD in the MEV for the period 2001-2010.

Figure captions

Figure 1. Study area.

Figure 2. Time evolution of HD in the MEV from 2001 to 2010.

Figure 3. From left to right: Geopotential height at 850 hPa in 2006, geopotential height average of period 2001-2010 and geopotential height average of period 1950-2010 (top: June; bottom: July).

Figure 4. From left to right: Geopotential height at 500 hPa in 2006, geopotential height average of period 2001-2010 and geopotential height average of period 1950-2010 (top: June; bottom: July).

Figure 5. From left to right: 850 hPa temperature difference between 2006 and 2001-2010 average; between 2006 and 1950-2010 average (top: June; bottom: July).

Figure 6. From left to right: Anomalies of temperature difference between 850 hPa and 500 hPa of 2006 respect to 2001-2010 average and 1950-2010 average (top: June; bottom: July).

Figure 7. Top: Decadal rate of change of 850 hPa temperature in the period 1950-2010 in June (left) and July (right). Bottom: Level of significance (1-〈).

Figure 8. Top: Decadal rate of change of 850 hPa geopotential height in the period 1950-2010 in June (left) and July (right). Bottom: Level of significance (1-〈).

Figure 9. 850 hPa temperature clusters for 1950-2010 period (left: June, right: July). Light grey color is Cluster 1 and dark grey color is Cluster 2.

Figure 10. From left to right: Continuous wavelet power spectrum of detrended time series of 850 hPa temperature in June (top) and July (bottom) for clusters 1 and 2, and the corresponding time series.

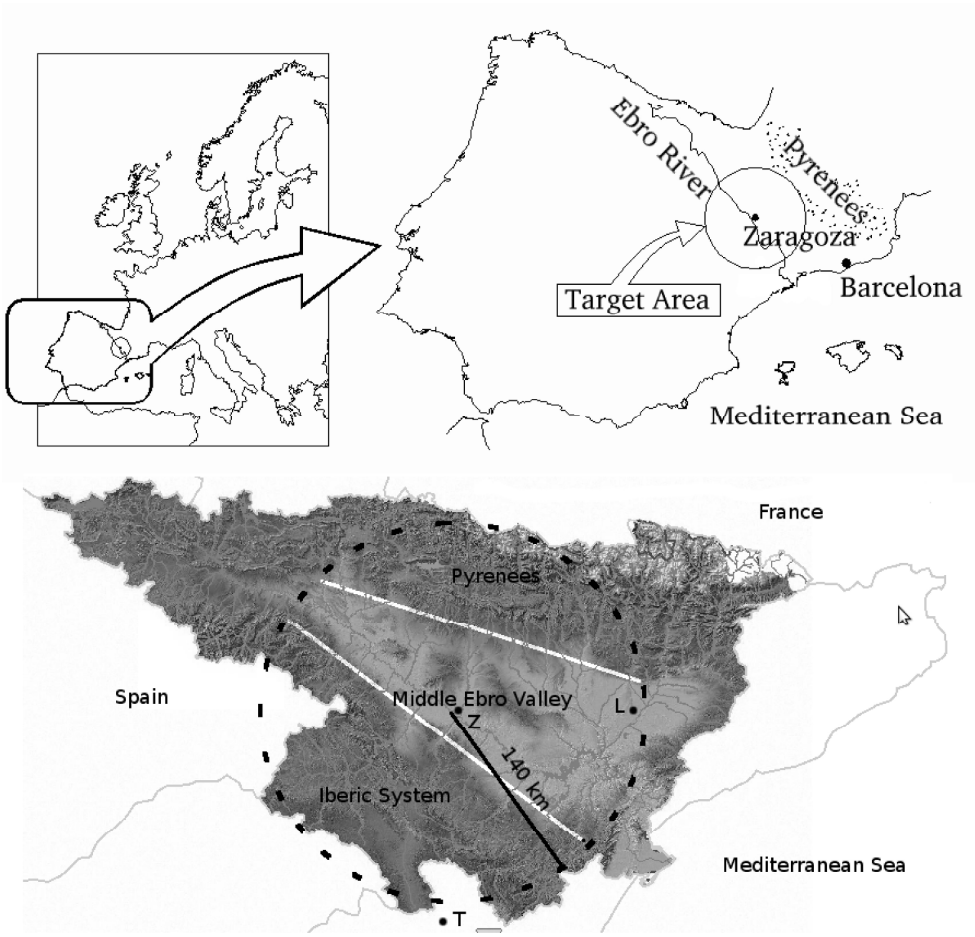

Study area.
300x287mm (300 x 300 DPI)

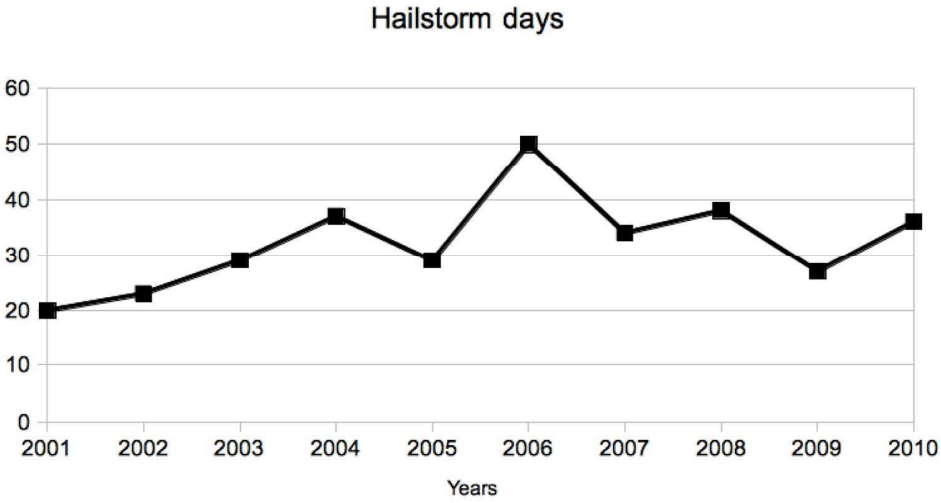

Time evolution of HD in the MEV from 2001 to 2010.
151x84mm (300 x 300 DPI)

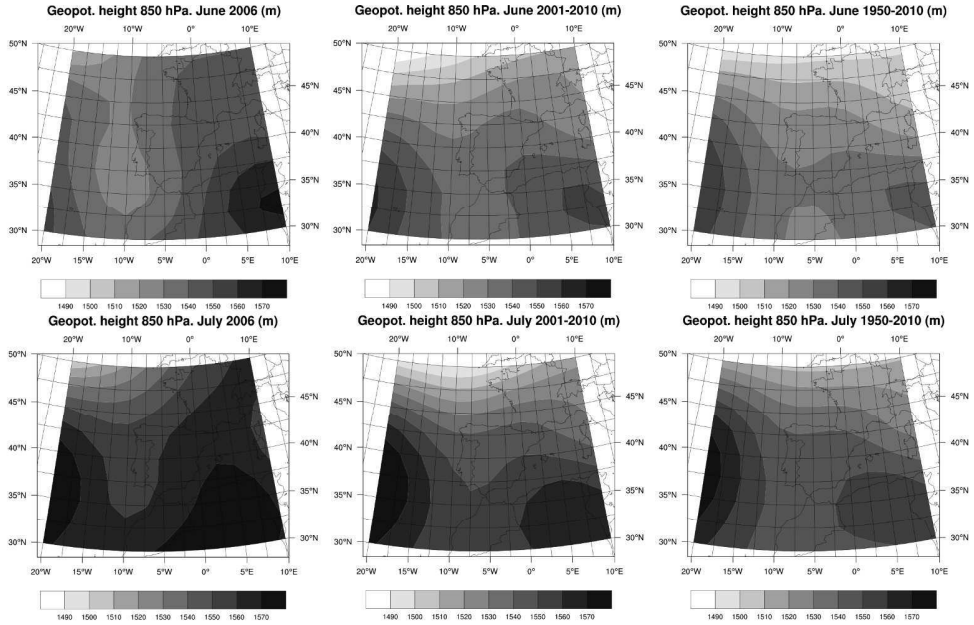

From left to right: Geopotential height at 850 hPa in 2006, geopotential height average of period 2001-2010 and geopotential height average of period 1950-2010 (top: June; bottom: July).
825x529mm (600 x 600 DPI)

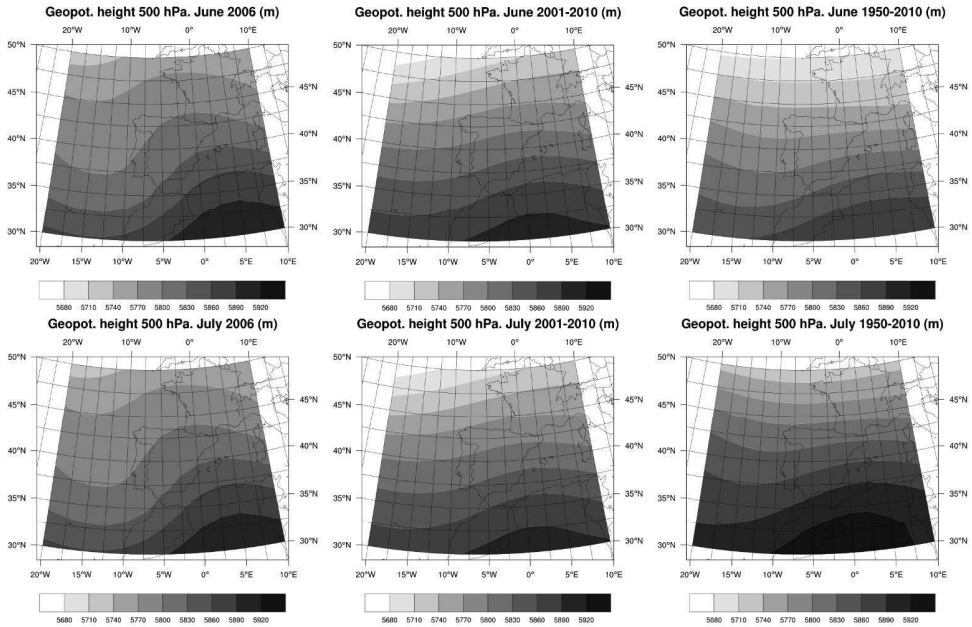

From left to right: Geopotential height at 500 hPa in 2006, geopotential height average of period 2001-2010 and geopotential height average of period 1950-2010 (top: June; bottom: July).
825x529mm (600 x 600 DPI)

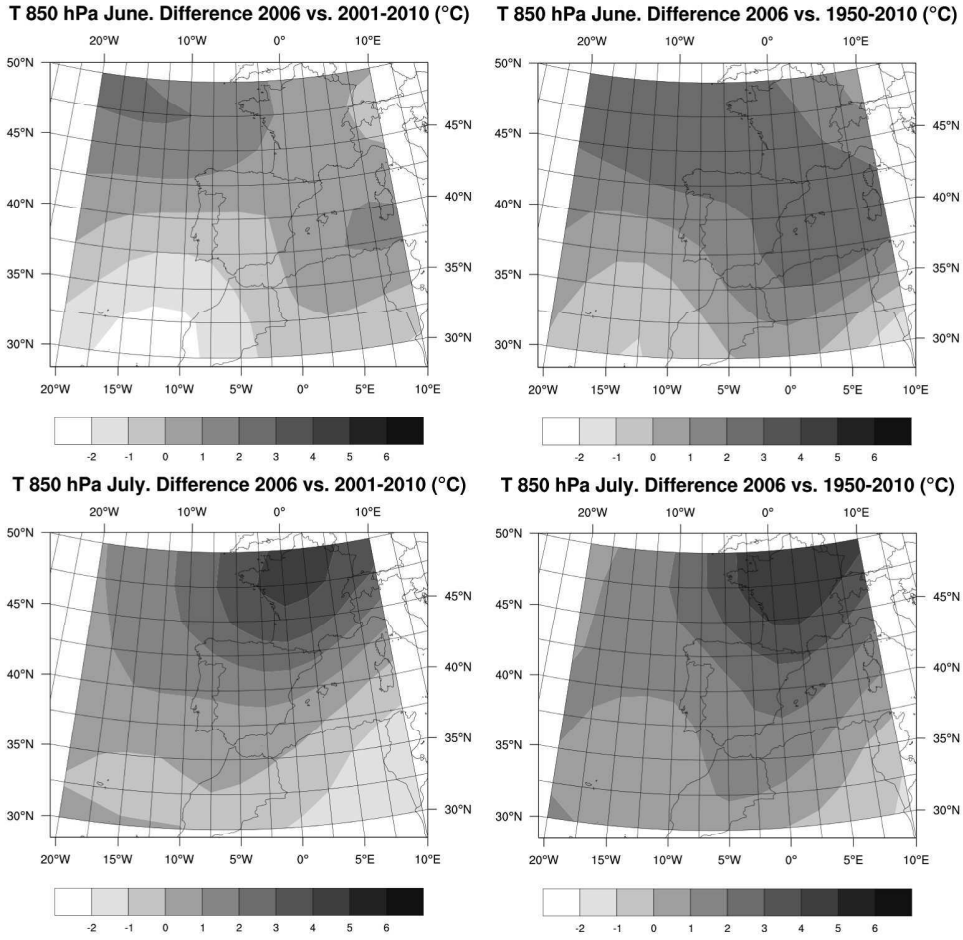

From left to right: 850 hPa temperature difference between 2006 and 2001-2010 average; between 2006 and 1950-2010 average (top: June; bottom: July).
550x529mm (600 x 600 DPI)

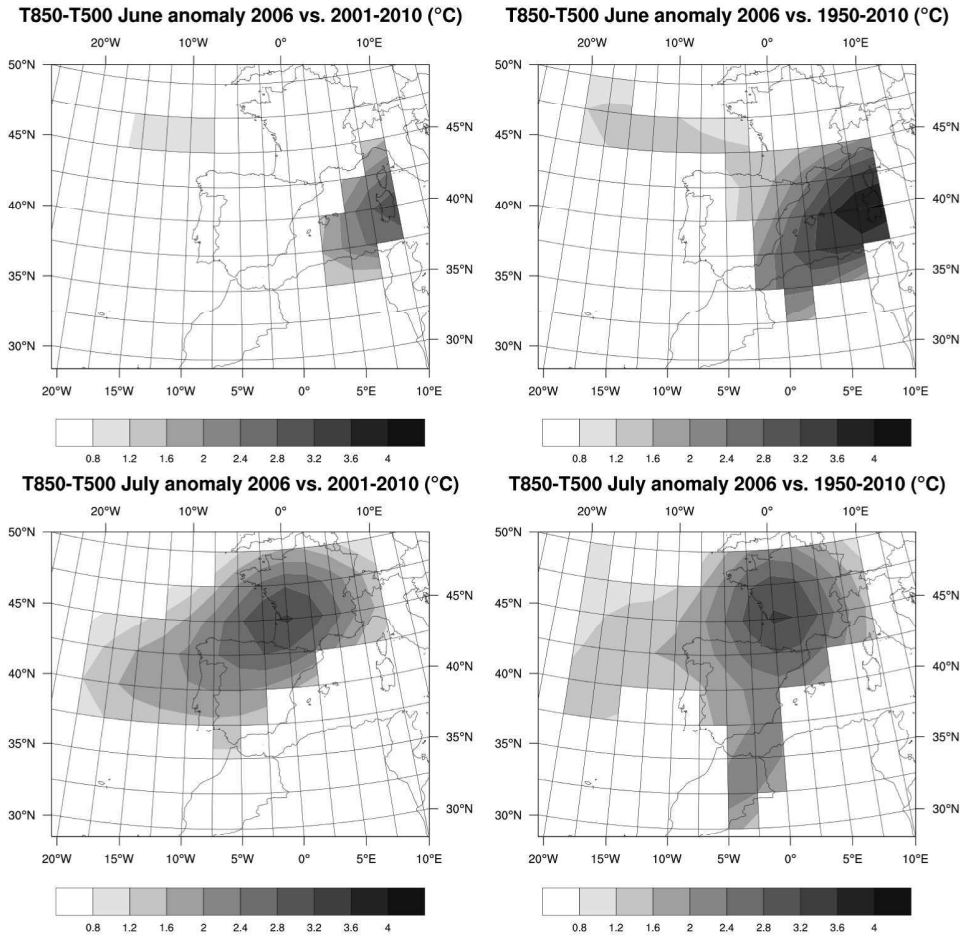

From left to right: Anomalies of temperature difference between 850 hPa and 500 hPa of 2006 respect to 2001-2010 average and 1950-2010 average (top: June; bottom: July).
550x529mm (600 x 600 DPI)

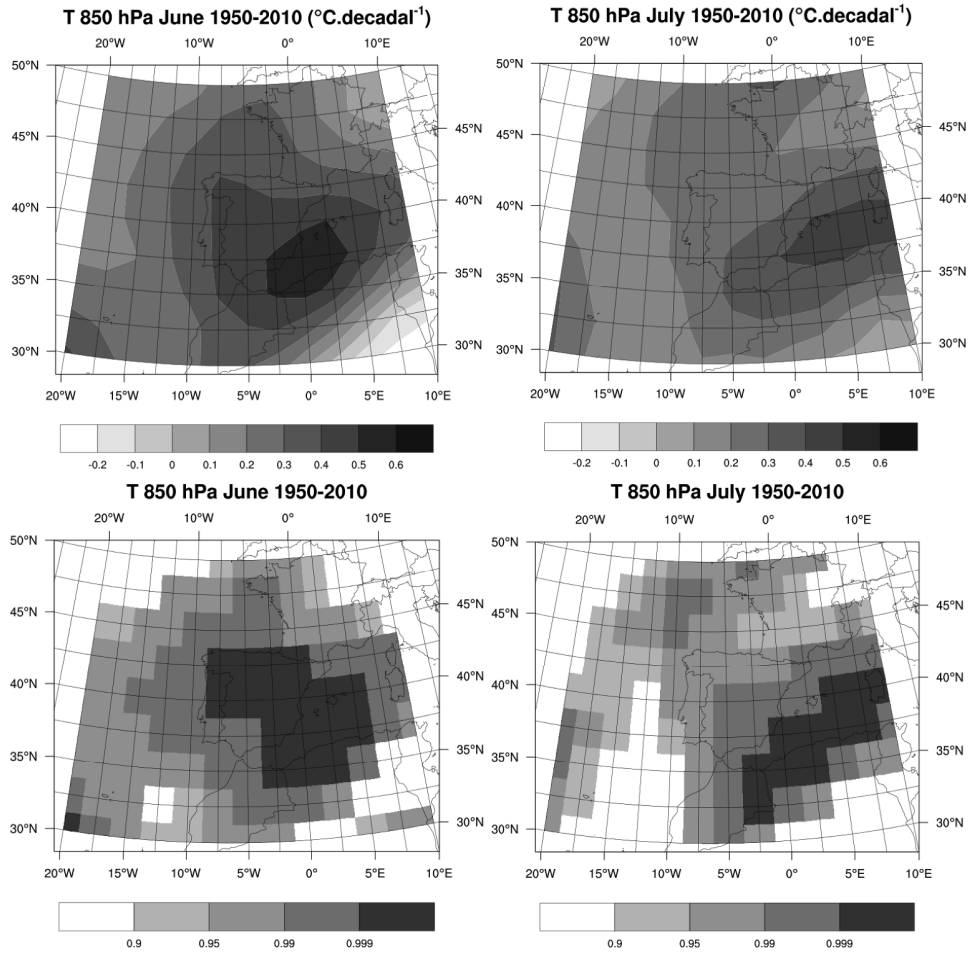

Top: Decadal rate of change of 850 hPa temperature in the period 1950-2010 in June (left) and July (right). Bottom: Level of significance (1-α).
381x373mm (300 x 300 DPI)

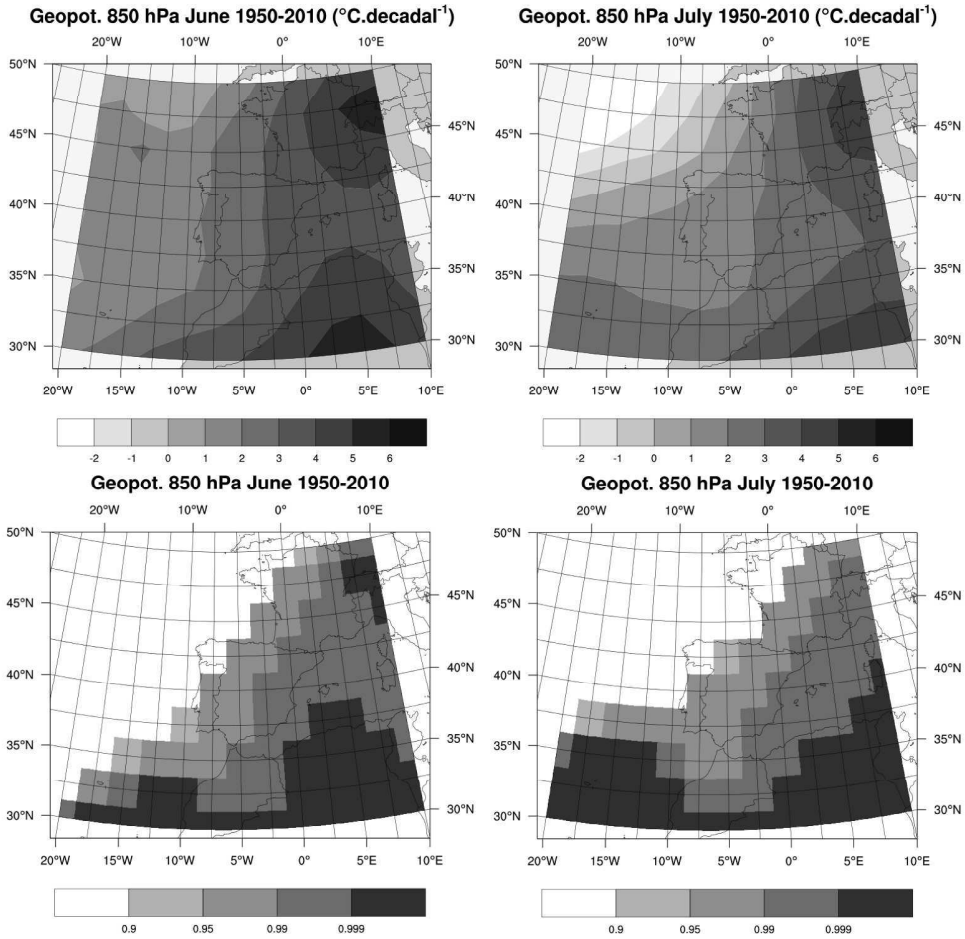

Top: Decadal rate of change of 850 hPa geopotential height in the period 1950-2010 in June (left) and July (right). Bottom: Level of significance (1-α).
547x548mm (600 x 600 DPI)

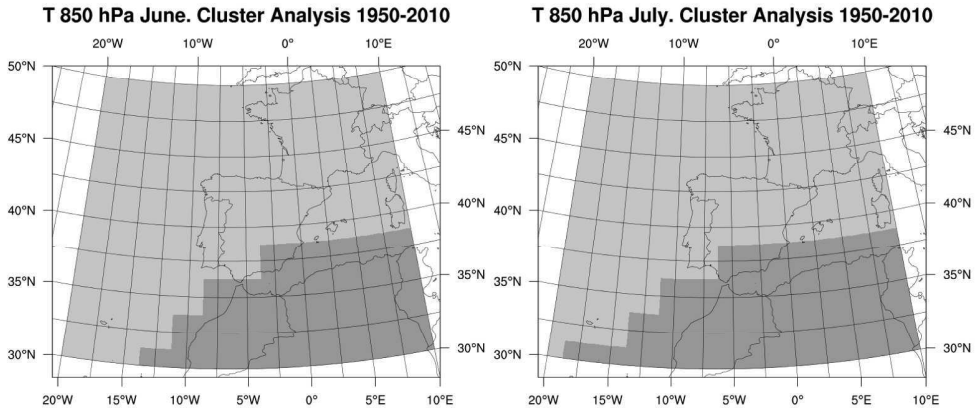

850 hPa temperature clusters for 1950-2010 period (left: June, right: July). Light grey color is Cluster 1 and dark grey color is Cluster 2.
241x105mm (300 x 300 DPI)

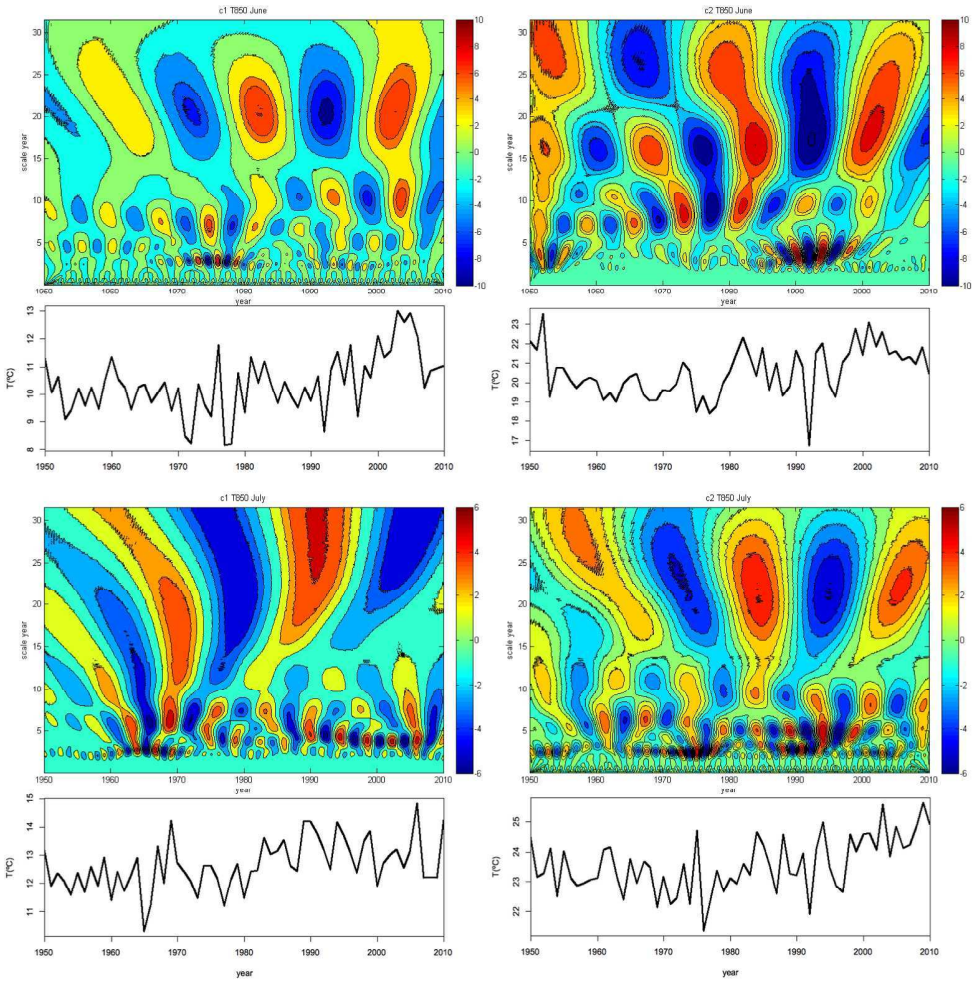

From left to right: Continuous wavelet power spectrum of detrended time series of 850 hPa temperature in June (top) and July (bottom) for clusters 1 and 2, and the corresponding time series.
550x560mm (600 x 600 DPI)